Original Paper

nephron
Physiology

Nephron Physiol 2007;105:p33–p41
DOI: 10.1159/000098136

Received: May 19, 2006
Accepted: October 13, 2006
Published online: December 28, 2006

Characterization of Two Novel Missense Mutations in the *AQP2* Gene Causing Nephrogenic Diabetes Insipidus

Achille Iolascon[a] Veruska Aglio[a] Grazia Tamma[b] Maria D'Apolito[a] Francesco Addabbo[b] Giuseppe Procino[b] Maria Carmela Simonetti[b] Giovanni Montini[d] Loreto Gesualdo[e] Erik W. Debler[f] Maria Svelto[b, c] Giovanna Valenti[b, c]

[a]Department of Biochemistry and Biomedical Technologies, University Federico II – CEINGE, Naples, [b]Department of General and Environmental Physiology, [c]Centro di Eccellenza in Genomica Comparata, University of Bari, Bari, [d]Clinica Pediatrica, University of Padua, Padua, [e]Department of Biomedical Science, Division of Nephrology, University of Foggia, Foggia, Italy; [f]Department of Molecular Biology and The Skaggs Institute for Chemical Biology, The Scripps Research Institute, La Jolla, Calif., USA

Key Words
Nephrogenic diabetes insipidus · Aquaporin · Polyuria

Abstract
Here, we report the aquaporin 2 *(AQP2)* mutational analysis of a patient with nephrogenic diabetes insipidus heterozygote due to two novel missense mutations. Direct sequencing of DNA in the male patient revealed that he was compound heterozygote for two mutations in the *AQP2* gene: a thymine-to-adenine transversion at position 450 (c.450T>A) in exon 2 and a guanine-to-thymine at nucleotide position 643 (c.643G>T) in exon 4. The double heterozygous 450T>A and 643G>T transversion causes the amino acid substitution D150E and G215C. Direct sequencing of exons 2 and 4 of the *AQP2* gene from each of the parents revealed that the c.450T>A mutation was inherited from the father while the c.643G>T mutation was inherited from the mother. Analysis of *AQP2* excretion demonstrated that no *AQP2* was detectable in the urine of the proband, whereas normal *AQP2* levels were measured in both parents. When expressed in renal cells, both proteins were retarded in the endoplasmic reticulum and no redistribution was observed after forskolin stimulation. Of note, homology modeling revealed that the two mutations involve two highly conserved residues providing important clues about the role of the wt residues in *AQP2* stability and function.

Introduction

Nephrogenic diabetes insipidus (NDI) is an inherited disease characterized by the failure of the kidney to concentrate urine in response to arginine vasopressin, because of a receptor or postreceptor defect. It is characterized by polyuria, polydipsia, fever, constipation, and acute hypernatremic dehydration after birth that may have neurological consequences. In most cases, the disease is X linked due to a mutation in the gene located on Xq28 coding for the V2 receptor of vasopressin (V2R) [1, 2]. The incidence of V2R NDI is 8.8 per million male births in Quebec [3]. Only males are symptomatic among patients with X-linked inheritance, while carrier females

KARGER

Fax +41 61 306 12 34
E-Mail karger@karger.ch
www.karger.com

1660–2137/07/1053–0033$23.50/0

Accessible online at:
www.karger.com/nep

Prof. Giovanna Valenti
Dipartimento di Fisiologia Generale e Ambientale
Via Amendola 165/A
IT–70126 Bari (Italy)
Tel. +39 080 544 344, Fax +39 080 544 3388, E-Mail g.valenti@biologia.uniba.it

sometimes present with mild NDI symptoms due to variable inactivation of the mutated gene. Most of the remaining forms of hereditary NDI are caused by mutations of the *aquaporin 2 (AQP2)* gene on chromosome 12 coding for the vasopressin-sensitive *AQP2* water channel [4, 5].

In response to vasopressin, *AQP2* is redistributed from intracellular storage vesicles to the apical membrane of collecting duct principal cells through activation of a cAMP signaling cascade [6, 7]. Protein kinase A-mediated phosphorylation of *AQP2* is essential in regulating the exocytosis of *AQP2*-containing vesicles, which renders the cells water permeable and allows water reabsorption driven by the corticomedullary osmotic gradient. This then leads to the formation of concentrated urine. Both recessive and dominant inheritance patterns of NDI have been reported. Recessive NDI can be caused by homozygosity for mutations in the *AQP2* gene. These mutations cause misfolding and consequential retention of *AQP2* in the endoplasmic reticulum (ER) [4, 8–11].

In dominant NDI, *AQP2* protein can either be retained in the Golgi network or sorted aberrantly to late endosomes/lysosomes or the basolateral membrane [12–17]. These mutants can form heterotetramers with wild-type *AQP2* protein but cannot translocate to the membrane in response to vasopressin. Identification of new *AQP2* mutations can help provide insight into critical regions in the *AQP2* protein, suggesting a pharmacological strategy for correcting the sorting defect [18–20].

In this study, we report a case of a human compound heterozygote for two previously unreported missense mutations in the *AQP2* gene encoding the *AQP2*-D150E and *AQP2*-G215C mutant proteins. To investigate whether either the *AQP2*-D150E or the *AQP2*-G215C protein can cause NDI in this patient, both proteins were separately expressed in polarized collecting duct epithelial cells and analyzed for their intracellular expression and routing in response to cAMP-elevating agents.

Materials and Methods

Analysis of the Patient with NDI

Blood and urine samples were collected from the patient and his parents in order to measure their osmolality; sodium concentrations were measured by standard procedures. Genomic DNA was obtained from the peripheral blood of the patient and his family by standard methods. PCR amplification of the *AQP2* gene was performed with primers described by Deen et al. [4, 21]. The amplified products were isolated by electrophoresis on a 1.5% agarose gel and then purified using the QIAamp purification kit (Qiagen), and the nucleotide sequence was determined by direct sequencing using an ABI 310 automatic sequencer according to the manufacturer's instructions (Applied Biosystem, Foster City, Calif., USA).

Constructs

The constructs encoding HA-pCDNA-*AQP2*-D150E and HA-pCDNA-*AQP2*-G215C were made by introducing the mutations into HA-pCDNA-*AQP2* with the *Pfu* DNA polymerase (Promega, Madison, Wisc., USA) using the following primers: APQ2_450T>A_F: cgcctccaccgaagagcgccgcggag; APQ2_450T>A_R: ctccgcggcgctcttcggtggaggcg; APQ2_643G>T_F: gcgccatcctgtgctccctcctctac; APQ2_643G>T_R: gtagaggagggagcacaggatggcgc.

PCR was performed on 50 μl (denaturation at 95°C for 30 s, annealing at 60°C for 45 s, and extension at 70°C for 7 min for 15 cycles). The PCR product was digested with 10 units of Dpn1, to degrade the methylated (parental) DNA. The digested and purified DNA was used to transform *Escherichia coli* bacterial cells. The accuracy of the mutated constructs was confirmed by DNA sequencing.

Analysis of Mutated AQP2 *Proteins*

The alignment of mutated proteins among various species was performed using ClustalW, a general-purpose multiple-sequence alignment program for DNA or proteins. It produces biologically meaningful multiple sequence alignments of divergent sequences. It calculates the best match for the selected sequences, and lines them up so that the identities, similarities and differences can be seen (http://www.ebi.ac.uk/clustalw/). The analysis of consensus regions for secondary modifications was performed using PROSITE, a database of protein families and domains (http://www.expasy.org/prosite/).

Analysis of AQP2 *Excretion*

An aliquot urine sample from the patient and his parents was used for *AQP2* excretion analysis by the enzyme-linked immunosorbent assay (ELISA) method. To this end, urine samples were spun down at 3,000 rpm for 10 min at 4°C to remove cellular debris in the presence of the following protease inhibitors: 2 mM phenylmethylsulphonyl fluoride, 1 μg/ml leupeptin, 1 μg/ml pepstatin. *AQP2* excretion was measured, as previously described, by ELISA [22]. Five or 10 μl of urine sample were diluted to 50 μl in PBS containing 0.01% SDS, placed in a MaxiSorp 96-well microplate (Nunc, Rochester, N.Y., USA) and incubated for 16 h at 4°C. In parallel wells, increasing concentrations (50, 100, 200, 300, 400, 500, 1,000 pg/50 μl) of a synthetic peptide reproducing the last 15 amino acids of the C-terminal region of the human *AQP2* were incubated as internal standard. Each sample was analyzed in triplicate. Wells were washed with washing buffer (PBS-0.1% Tween 20) and incubated with a PBS blocking solution containing 3% BSA at room temperature for 1 h. Ten micrograms of affinity purified anti-*AQP2* antibodies was diluted in blocking solution (final antibody dilution 1:1,000) and 50 μl of solution were then added to each well and incubated for 3 h at 37°C. The wells were then washed with washing buffer, and antirabbit IgG conjugated with horseradish peroxidase (1:5,000; Sigma) was added to each well and incubated for 1 h at 37°C. After five washings with washing buffer, 50 μl of the substrate solution [2, 2′-azino-bis(3-ethylbenzthiazoline-6-sulfonic acid); Sigma] were

added to each well and incubated for 30 min in the dark. Absorbance was measured with a microplate reader (BioRad, model 550) at 405 nm.

Cell Culture and Transfections

Mouse cortical collecting duct M-1 cells [23], originating from mice transgenic for the early region of simian virus 40, were purchased from the European Collection of Cell Culture, cultured in DMEM/F12 1:1 supplemented with 2 mM glutamine, 5 μM dexamethasone, 5% fetal calf serum until they were about 95% confluent and then transfected with a plasmid encoding wild-type human *AQP2*. Lipofectamine 2000 (Life Technologies, San Giuliano Milanese, Italy) was used to transfect cells according to manufacturer's instructions.

After transfection, cells were grown for 2 days and then trypsinized and transferred to 10-mm dishes. A selection of cells containing transfected DNA was obtained with a culture medium containing Geneticin (500 μg/ml, Life Technologies, Inc.) for 10–15 days. Resistant clones were isolated and transferred for expansion and analysis. One of these clones, referred to as MCD4, was used in subsequent studies.

M-1 cells were also transiently transfected with the two plasmids HA-pCDNA-*AQP2*-D150E or HA-pCDNA-*AQP2*-G215C. Cells were processed for immunofluorescence microscopy or Western blotting 48 h after transfection.

Immunofluorescence and Western Blot Analysis

MCD4 cells, stably transfected with wild-type human *AQP2* and M-1 cells, transiently transfected with HA-pCDNA-*AQP2*-D150E or HA-pCDNA-*AQP2*-G215C were grown to confluence on porous cell culture inserts (Becton Dickinson Labware, USA) and treated with or without 10^{-4} M forskolin (FK) for 20 min at 37°C before being fixed with 3% PFA with 0.1% Triton X-100 for 20 min at room temperature. After blocking in 0.1% gelatin in PBS for 20 min, cells were incubated at room temperature for 1 h with *AQP2* affinity-purified antibodies and with anti-calnexin antibodies (1:100; Santa Cruz Biotechnology).

Cells were washed with 0.1% gelatin in PBS and incubated for 60 min with donkey antirabbit IgG Alexa Fluor 488 and donkey antigoat IgG Alexa Fluor 546 (both diluted 1:1,000), followed by washing twice for 1 min in high-salt PBS and twice in regular PBS. The filters were then removed, mounted and *AQP2* and calnexin were detected with a confocal microscope (Leica TCS SP2, Leica Microsystems).

For lysate preparations, cells were washed in PBS and resuspended in ice-cold lysis buffer containing 50 mM Tris, 110 mM NaCl, 0,5% Triton X-100, 0.5% Nonidet P-40, and 2 mM phenylmethylsulfonyl fluoride and proteases inhibitor cocktail, pH 8. Cell suspension was incubated on ice for 1 h and vortexed several times. Insoluble material was pelleted at 11,000 *g*, and protein content was determined by the method of Lowry [24]. Sixty micrograms of cell lysate was dissolved in SDS loading buffer, heated to 60°C for 10 min, and separated by electrophoresis on 13% SDS-polyacrylamide gel electrophoresis and transferred onto Immobilon-P membrane. To check the efficiency of the transfer, the membrane was briefly stained with Coomassie Blue, destained, blocked in blotting buffer containing 5% nonfat dry milk, 150 mM NaCl, 1% Triton X-100, and 20 mM Tris-HCl, pH 7.4, for 60 min and incubated overnight with affinity purified anti-*AQP2* antibodies (1:500 diluted in blotting buffer). Membranes were then washed in several changes of blotting buffer and incubated for 60 min with alkaline phosphatase-conjugated secondary antibody (1:30,000; Sigma) and visualized using the 1-Step NBT/BCIP detection system (Pierce).

Homology Modeling

For homology modeling, bovine aquaporin 0 (pdb code 1YMG) was identified as the best target since it displayed the highest E value (1e-75) and high sequence identity (60%) in sequence alignment in BLAST (http://www.ncbi.nlm.nih.gov/blast/) using proteins of known 3-D structure. Alignment was improved by ClustalW. The homology models were obtained from the SWISS-MODEL server (http://swissmodel.expasy.org//SWISS-MODEL.html) and visualized in PyMOL (http://www.pymol.org).

Results

Clinical Evaluation of the Patient with NDI

The male patient was referred to the Pediatric Department of Padua University at the age of 9 months because of vomiting, failure to thrive, polydipsia and polyuria. He was the second child of nonconsanguineous parents and had a healthy brother. Family history was negative for NDI. Blood and urine analyses revealed a natremia of 141,3 mM, plasmatic osmolality of 281 mosm/kg, urinary osmolality of 80 mosm/l and body weight 6.91 kg. The diagnosis of diabetes insipidus was made by the Miller test: restriction of liquids followed by intranasal administration of vasopressin. The patient showed a maximal urine osmolality of 202 mosm/kg after 12-hour thirsting with serum Na 152, plasma osmolality of 299 mosm/kg, plasma ADH values > 64 ng/l (NV: 5–11) and an 8% decrease in weight. DDAVP was then given (intranasal, 2 puffs of 0.1 mg each) resulting in the following osmolality values: 252 (1 ml), 156 (55 ml), 137 (75 ml) and 89 (60 ml) 1, 2, 3 and 4 h after the administration of the DDAVP.

The patient with NDI along with his parents and brother were analyzed by direct sequencing in the whole coding sequence and the splice sites of the *AQP2* gene. Direct sequencing of DNA in the patient revealed that he was compound heterozygote for two previously unreported missense mutations in the *AQP2* gene; a thymine-to-adenine transversion at position 450 (c.450T>A) in exon 2 and a guanine-to-thymine at nucleotide position 643 (c.643G>T) in exon 4, resulting in an aspartic acid-to-glutamic acid substitution at codon 150 (D150E) and glycine-to-cysteine substitution at codon 215 (G215C), respectively (fig. 1). (Recommendations for the description of DNA sequence variants: http://www.hgvs.org/mutnomen/recs-DNA.html#sub.) Both D150 and G215

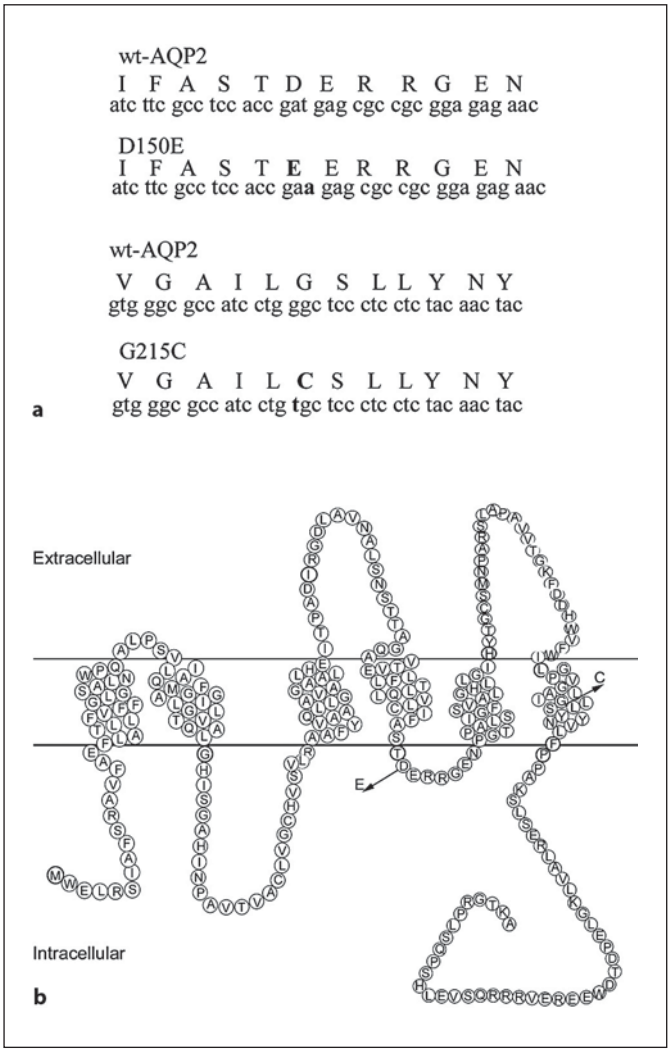

Fig. 1. a Comparison between the wt-*AQP2* and its mutants. The amino acids and the corresponding nucleotide sequences of wt-*AQP2*, D150E and G215C mutants are shown. The identified mutations are in bold. **b** Localization of the mutations in *AQP2*. The two missense mutations, as identified in the NDI patient, are indicated.

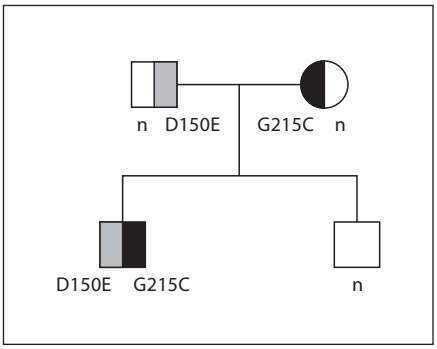

Fig. 2. Inheritance of NDI in the analyzed family. The affected male (square) was heterozygotic for two previously unreported missense mutations in the *AQP2* gene, the D150E inherited from the father and the G215C inherited from the mother (circle). By contrast, his healthy brother inherited both of the normal (n) alleles from the parents.

Table 1. Principal clinical parameters in the NDI patient and his parents

Parameters	Father	Mother	Affected child
Diuresis, ml/24 h	1,050	1,250	2,150
Creatinine, mg/dl	253.1	120.9	5.7
Osmolality, mosmol/kg	1,080	580	80
AQP2, fmol/ml	2,349 ± 258	3,430 ± 211	n.d.
AQP2/creatinine, fmol/mg	928 ± 102	2,837 ± 174	n.d.

Values are expressed as mean ± SE; n.d. = not detectable.

are highly conserved among various species. Direct sequencing of exon 2 and exon 4 from the *AQP2* gene of each parent revealed that the c.450T>A mutation was inherited from the father while the c.643G>T mutation was inherited from the mother. The healthy brother presented both normal alleles (fig. 2). Sequencing of the PCR products of the exon 2 and exon 4 coding region of 100 normal chromosomes from a control group indicated that the missense mutations identified in this study were not present in the normal population.

Urinary Excretion of AQP2

The principal clinical parameters related to the patient and his parents are summarized in table 1. The patient had dramatically increased urine production (2,150 ml/day) compared to his heterozygotic parents. Consistent with these data, the affected child's urine osmolality was very low (80 mosm/kg). *AQP2* excretion from the patient and from his parents was evaluated by ELISA as described in the 'Materials and Methods' section. It has been demonstrated that this method can detect as low as 5.6 fmol of urinary *AQP2* [25]. The *AQP2* concentration obtained from the mother and father were 2,837 ± 174 and 928 ± 102 fmol/ml, respectively. In the affected child, *AQP2* excretion was below the sensitivity of the assay.

Since the absence of *AQP2* signal obtained by the ELISA might be due to dilution by polyuria, *AQP2* excretion was also evaluated by Western blotting as described by Valenti et al. [26]. A total of 150 mg of creatinine equivalent of each sample was processed and subjected to immunoblot analysis to semiquantify the amount of *AQP2* in the sample. Although a clear *AQP2* band was visible in the lanes loaded with healthy parents' urine, no bands were detected in the lanes loaded with patient's urine (data not shown).

Expression Analysis of AQP2-*D150E and* AQP2-*G215C in Collecting Duct Cells*

To determine whether the identified mutations could be causal for NDI in this patient, each mutation was introduced into the *AQP2* cDNA sequence, cloned into an expression vector. The plasmids obtained were transiently transfected in M-1 mouse collecting duct cells not expressing the water channel *AQP2* [23]. Cells expressing both *AQP2* mutants, along with MCD4 cells, stably transfected with wt-*AQP2*, were then lysated and subjected to immunoblotting studies. For the *AQP2* mutants *AQP2*-D150E and *AQP2*-G215C, the unglycosylated 29-kDa and high-mannose glycosylated 32-kDa forms were present, characteristic for ER-retained *AQP2* proteins, whereas a 29-kDa band and a 40- to 45-kDa glycosylated band (Gly) were detected for wt-*AQP2* (fig. 3).

Immunofluorescence experiments of transiently transfected cells showed typical intracellular vesicles staining for wt-*AQP2*, which redistributed to the plasma membrane upon FK stimulation. By contrast, in cells transfected with mutant *AQP2*-D150E or *AQP2*-G215C, a scattered intracellular expression was observed in the absence and in the presence of FK stimulation (fig. 4), which strongly colocalized with the ER marker calnexin (fig. 4; merge). Confocal scanning of the intracellular staining performed in single cells along the z-axes (fig. 4; z-scan) confirmed a low degree of colocalization between wt-*AQP2* and calnexin along with a clear redistribution of wt-*AQP2* staining from an intracellular compartment towards the apical membrane after FK stimulation. In contrast, the same analysis revealed a strong colocalization of both *AQP2*-D150E and *AQP2*-G215C with calnexin, consisting in retention of both mutated proteins in the ER, and no redistribution of both *AQP2* mutants staining in the presence of FK.

3-D Homology Modeling of AQP2 *and Its Mutations*

The overall structure of the wt-*AQP2* model strongly resembles its parent model, bovine AQP0, as evidenced by low RMS deviations (0.2 Å; fig. 5a). In combination with good geometry and the lack of clashes within the model, these results indicate that the obtained *AQP2* structure represents a plausible model of *AQP2* and provides a solid basis to discuss the implications of the two observed mutations on the molecular level. D150 is located at the cytoplasmic end of helix H4 (fig. 5a). Its carboxylate group maximizes its hydrogen bond acceptor potential by engaging in four hydrogen bonds with the backbone NH of R152, the guanidinium group of R152, and with the hydroxyl group of Y219 from helix H6, all of which are formed with perfect geometry (fig. 5b). The high sequence conservation of D150, R152, and Y219 underscores the important structural role of this hydrogen bond network in aquaporins. In contrast, the *AQP2*-D150E mutant would be unable to form this finely tuned hydrogen bond network; E150 would make only a single hydrogen bond with R152. Mutation G215C occurs in the middle of the transmembrane region of H6 facing H4 (fig. 5 a, c). G215 corresponds to the last residue in the conserved sequence pattern GPxxGxxxG. In general, the GxxxG motif is the most frequently occurring sequence motif in transmembrane domains and mediates high-affinity helix-helix association [27]. Mutation of glycine in this motif is reported to result in strong de-

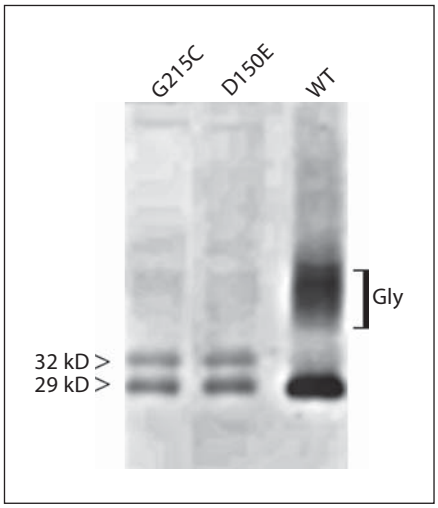

Fig. 3. Expression of *AQP2* in collecting duct renal cells transiently transfected with human D150E or G215C *AQP2* mutants. Control MCD4 cells, stably transfected with WT *AQP2*, were used as positive control (WT). Cells were lysated and subjected to immunoblotting analysis for *AQP2*. Unglycosylated *AQP2* (29 kDa), high-mannose glycosylated *AQP2* (32 kDa) and mature 35- to 45-kDa glycosylated *AQP2* bands (Gly) are indicated.

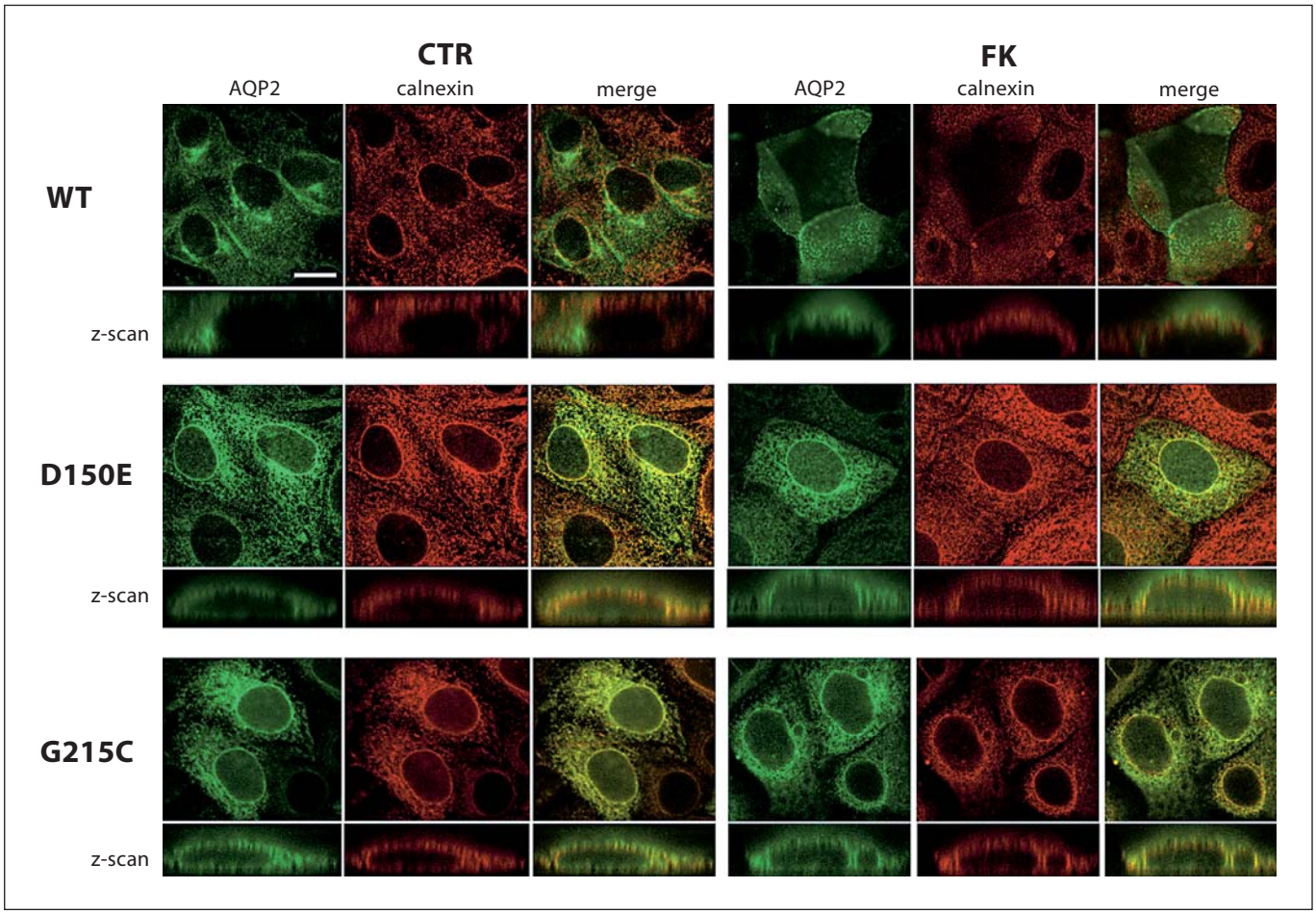
CTR
FK
AQP2
calnexin
merge
AQP2
calnexin
merge
WT
z-scan
D150E
z-scan
G215C
z-scan

4

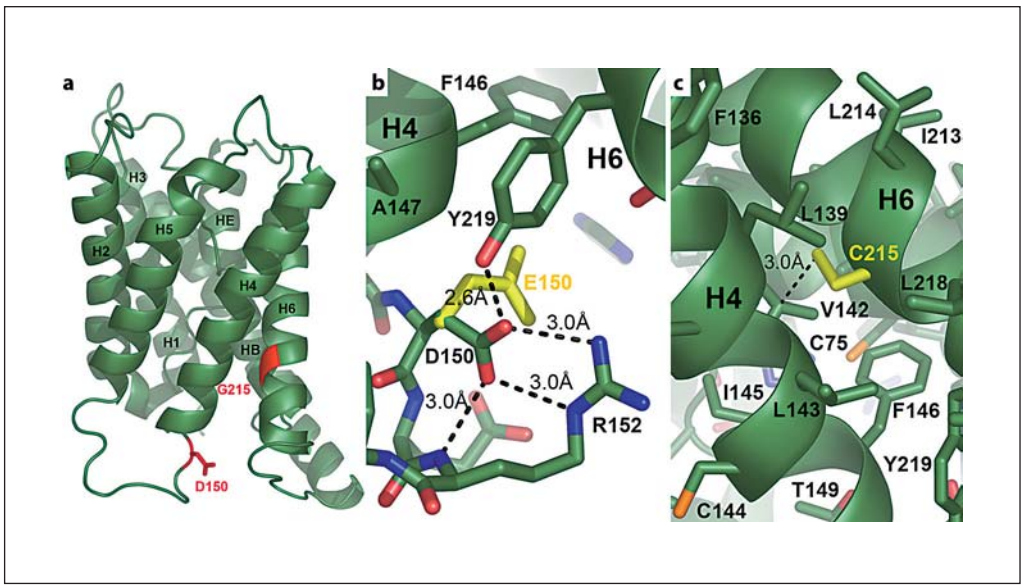
a
H3
H5
HE
H2
H4
H6
H1
HB
G215
D150
b
F146
H4
H6
A147
Y219
E150
2.6Å
3.0Å
D150
3.0Å
3.0Å
R152
c
F136
L214
I213
H6
L139
C215
3.0Å
L218
H4
V142
C75
I145
L143
F146
Y219
T149
C144

5

stabilization of helix-helix association by steric clashes, by a significant increase in the side chain entropy, and by a decrease in electrostatic complementarity [27]. In agreement with these findings, C215 would undergo unfavorable close contacts with V142 and the polar cysteine would be embedded in a highly hydrophobic environment, thus destabilizing the mutant protein. Finally, formation of disulfide bridges with C144 or C75, which are in immediate vicinity (<10 Å) to C215, would be another plausible mechanism for disruption of the aquaporin structure.

Discussion

In this study, we identified a case of a heterozygote patient with two previously unreported missense mutations in the *AQP2* gene causing NDI. While family history was negative for NDI, direct sequencing of DNA in the male patient of exon 2 and exon 4 of the *AQP2* gene revealed that the c.450T>A mutation was inherited from the father while the c.643G>T mutation was inherited from the mother. These mutations result in an aspartic acid-to-glutamic acid substitution at codon 150 (D150E) and glycine-to-cysteine substitution at codon 215 (G215C), respectively. The healthy brother presented both normal alleles.

In recessive NDI, nonfunctional mutants are thought to be retained in the ER and fail to tetramerize, while *AQP2* mutants responsible for dominant NDI oligomerize with the product of the wild-type allele forming tetramers that are improperly targeted and do not reach the apical cell surface [15, 28]. Upon expression in collecting duct cells, both *AQP2*-D150E and *AQP2*-G215C appeared to be retained in the ER, as a 32-kDa high-mannose glycosylated band, characteristic of ER-retarded *AQP2* mutants in recessive NDI, was observed [4, 15, 29]. Consistently, immunolocalization studies of both *AQP2*-D150E and *AQP2*-G215C displayed a high degree of colocalization with calnexin, a specific ER marker. Finally, FK treatment did not change the intracellular localization of both mutated proteins, indicating that they are impaired in their trafficking to the plasma membrane in response to cAMP-elevating agents.

Our data indicate that, similarly to other *AQP2* mutants in recessive NDI, both the encoded *AQP2*-D150E and *AQP2*-G215C cause recessive NDI because of ER retention as demonstrated by confocal analysis of the colocalization for both mutants with the ER marker calnexin when expressed in a collecting duct cell line. This hypothesis is corroborated by the absence of mutant *AQP2* proteins in patient's urine whereas *AQP2* was easily detected in the urine of his healthy parents.

Strict conservation of helical tertiary structure in aquaporins and high sequence identity of human *AQP2* with other aquaporins encouraged us to construct 3-D homology models of *AQP2* and its two mutants in order to understand the cellular consequences on the molecular level. The two mutations involve two highly conserved residues which play important structural roles in aquaporins. Homology modeling suggests that both E150 and C215 would considerably disrupt the favorable interactions of the wt-residues, resulting in significant destabilization of the mutant proteins. Since the affected helices H4 and H6 are in contact with other aquaporin monomers in the tetramer, the structural changes may ultimately obstruct quaternary structure assembly or lead to unstable or unfunctional heterotetramers in the patient. Therefore, the mutant *AQP2* are likely to be subject to ER-associated protein degradation [12] which eliminates misfolded or unassembled proteins from the ER [30], consistent with the experimentally found ER retention. It is likely that mutated proteins are not stable because they are impaired in the interaction with ER molecular chaperones [31, 32].

Fig. 4. Localization of *AQP2* mutants in renal collecting duct cells. Collecting duct renal cells transfected with wt-*AQP2*, *AQP2*-D150E or *AQP2*-G215C were grown to confluence, incubated in the absence or in the presence of FK, fixed and immunostained using antihuman *AQP2* and anticalnexin antibodies as a marker for the ER. *AQP2* is visualized with Alexa Fluor 488 (green), whereas calnexin is visualized with Alexa Fluor 546 (red). *AQP2*-D150E- and *AQP2*-G215C-expressing cells showed a diffused cytoplasmic staining overlapping with that obtained with the ER marker calnexin (merge), which is consistent with ER retention for both mutants. Confocal scanning of the staining along the z-axis showed that no change in the staining was observed after FK stimulation for either mutants, whereas wt-*AQP2* redistributed to the apical pole of the cell (z-scan). Bar = 10 μm.

Fig. 5. Homology model of *AQP2* and its mutants. **a** Cartoon of wt-*AQP2*. The helices are labeled according to Murata et al. [33]. Residues D150 and G215, each of which are mutated in the two mutant forms of *AQP2*, are highlighted in red. **b** Close view of the highly conserved D150 and its hydrogen bond interactions. The mutation D150E (yellow) fails to form an equivalent hydrogen bond network, thus destabilizing *AQP2*. **c** Close view of the region around the well-conserved residue G215, which allows close interhelical packing of H4 and H6. Mutation to the polar residue C215 (yellow) in the highly hydrophobic environment results in unfavorable steric and electrostatic interactions with neighboring residues. Disulfide bridge formation with C75 or C144 may obstruct proper folding into the wt-tertiary structure.

To conclude, we have identified a case of a human heterozygote for two previously unreported missense mutations in the *AQP2* gene causing NDI. Our data indicate that both *AQP2* missense mutations lead to ER retention. Since the quality control system for properly folded proteins is located in the ER, this result suggests that *AQP2* may be misfolded or misassembled. Furthermore, the two naturally occurring mutations in *AQP2* provide important clues about the role of the wt-residues in *AQP2* stability and function, which should hold true for other aquaporins as well. Lastly, our findings motivate more experiments to elucidate the fate and oligomerization state of the ER-retained *AQP2* mutants.

Acknowledgments

We wish to thank Anthony Green for proofreading and providing linguistic advice.

This work was supported by funds from Telethon (project GGP04202 to G.V.); from the Italian 'Ministero della Ricerca Scientifica e Tecnologica', COFIN-PRIN 2004 to G.V.; from the Centro di Eccellenza di Genomica in campo Biomedico ed Agrario, and from the Laboratorio Analisi del Gene.

References

1 Bichet DG: Nephrogenic diabetes insipidus. Adv Chronic Kidney Dis 2006;13:96–104.

2 Fujiwara TM, Bichet DG: Molecular biology of hereditary diabetes insipidus. J Am Soc Nephrol 2005;16:2836–2846.

3 Arthus MF, Lonergan M, Crumley MJ, Naumova AK, Morin D, De Marco LA, Kaplan BS, Robertson GL, Sasaki S, Morgan K, Bichet DG, Fujiwara TM: Report of 33 novel AVPR2 mutations and analysis of 117 families with X-linked nephrogenic diabetes insipidus. J Am Soc Nephrol 2000;11:1044–1054.

4 Deen PM, Croes H, van Aubel RA, Ginsel LA, van Os CH: Water channels encoded by mutant aquaporin-2 genes in nephrogenic diabetes insipidus are impaired in their cellular routing. J Clin Invest 1995;95:2291–2296.

5 Mulders SM, Knoers NV, Van Lieburg AF, Monnens LA, Leumann E, Wuhl E, Schober E, Rijss JP, Van Os CH, Deen PM: New mutations in the AQP2 gene in nephrogenic diabetes insipidus resulting in functional but misrouted water channels. J Am Soc Nephrol 1997;8:242–248.

6 Brown D: The ins and outs of aquaporin-2 trafficking. Am J Physiol Renal Physiol 2003;284:F893–F901.

7 Valenti G, Procino G, Tamma G, Carmosino M, Svelto M: Minireview: aquaporin 2 trafficking. Endocrinology 2005;146:5063–5070.

8 Canfield MC, Tamarappoo BK, Moses AM, Verkman AS, Holtzman EJ: Identification and characterization of aquaporin-2 water channel mutations causing nephrogenic diabetes insipidus with partial vasopressin response. Hum Mol Genet 1997;6:1865–1871.

9 Pasel K, Schulz A, Timmermann K, Linnemann K, Hoeltzenbein M, Jaaskelainen J, Gruters A, Filler G, Schoneberg T: Functional characterization of the molecular defects causing nephrogenic diabetes insipidus in eight families. J Clin Endocrinol Metab 2000;85:1703–1710.

10 van Lieburg AF, Verdijk MA, Knoers VV, van Essen AJ, Proesmans W, Mallmann R, Monnens LA, van Oost BA, van Os CH, Deen PM: Patients with autosomal nephrogenic diabetes insipidus homozygous for mutations in the aquaporin 2 water-channel gene. Am J Hum Genet 1994;55:648–652.

11 Vargas-Poussou R, Forestier L, Dautzenberg MD, Niaudet P, Dechaux M, Antignac C: Mutations in the vasopressin V2 receptor and aquaporin-2 genes in 12 families with congenital nephrogenic diabetes insipidus. J Am Soc Nephrol 1997;8:1855–1862.

12 Asai T, Kuwahara M, Kurihara H, Sakai T, Terada Y, Marumo F, Sasaki S: Pathogenesis of nephrogenic diabetes insipidus by aquaporin-2 C-terminus mutations. Kidney Int 2003;64:2–10.

13 de Mattia F, Savelkoul PJ, Kamsteeg EJ, Konings IB, van der Sluijs P, Mallmann R, Oksche A, Deen PM: Lack of arginine vasopressin-induced phosphorylation of aquaporin-2 mutant AQP2-R254L explains dominant nephrogenic diabetes insipidus. J Am Soc Nephrol 2005;16:2872–2880.

14 Kamsteeg EJ, Bichet DG, Konings IB, Nivet H, Lonergan M, Arthus MF, van Os CH, Deen PM: Reversed polarized delivery of an aquaporin-2 mutant causes dominant nephrogenic diabetes insipidus. J Cell Biol 2003;163:1099–1109.

15 Marr N, Bichet DG, Hoefs S, Savelkoul PJ, Konings IB, De Mattia F, Graat MP, Arthus MF, Lonergan M, Fujiwara TM, Knoers NV, Landau D, Balfe WJ, Oksche A, Rosenthal W, Muller D, Van Os CH, Deen PM: Cell-biologic and functional analyses of five new aquaporin-2 missense mutations that cause recessive nephrogenic diabetes insipidus. J Am Soc Nephrol 2002;13:2267–2277.

16 Mulders SM, Bichet DG, Rijss JP, Kamsteeg EJ, Arthus MF, Lonergan M, Fujiwara M, Morgan K, Leijendekker R, van der Sluijs P, van Os CH, Deen PM: An aquaporin-2 water channel mutant which causes autosomal dominant nephrogenic diabetes insipidus is retained in the Golgi complex. J Clin Invest 1998;102:57–66.

17 Procino G, Carmosino M, Marin O, Brunati AM, Contri A, Pinna LA, Mannucci R, Nielsen S, Kwon TH, Svelto M, Valenti G: Ser-256 phosphorylation dynamics of aquaporin 2 during maturation from the ER to the vesicular compartment in renal cells. FASEB J 2003;17:1886–1888.

18 Marr N, Kamsteeg EJ, van Raak M, van Os CH, Deen PM: Functionality of aquaporin-2 missense mutants in recessive nephrogenic diabetes insipidus. Pflugers Arch 2001;442:73–77.

19 Noda Y, Sasaki S: Molecular mechanisms and drug development in aquaporin water channel diseases: molecular mechanism of water channel aquaporin-2 trafficking. J Pharmacol Sci 2004;96:249–254.

20 Tamarappoo BK, Verkman AS: Defective aquaporin-2 trafficking in nephrogenic diabetes insipidus and correction by chemical chaperones. J Clin Invest 1998;101:2257–2267.

21 Deen PM, Verdijk MA, Knoers NV, Wieringa B, Monnens LA, van Os CH, van Oost BA: Requirement of human renal water channel aquaporin-2 for vasopressin-dependent concentration of urine. Science 1994;264:92–95.

22 Valenti G, Fraszl W, Addabbo F, Tamma G, Procino G, Satta E, Cirillo M, De Santo NG, Drummer C, Bellini L, Kowoll R, Schlemmer M, Vogler S, Kirsch KA, Svelto M, Gunga HC: Water immersion is associated with an increase in aquaporin-2 excretion in healthy volunteers. Biochim Biophys Acta 2006;1758:1111–1116.

23 Fejes-Toth G, Naray-Fejes-Toth A: Differentiation of renal beta-intercalated cells to alpha-intercalated and principal cells in culture. Proc Natl Acad Sci USA 1992;89:5487–5491.
24 Lowry OH, Rosebrough NJ, Farr AL, Randall RJ: Protein measurement with the folin phenol reagent. J Biol Chem 1951;193:265–275.
25 Umenishi F, Summer SN, Cadnapaphornchai M, Schrier RW: Comparison of three methods to quantify urinary aquaporin-2 protein. Kidney Int 2002;62:2288–2293.
26 Valenti G, Laera A, Pace G, Aceto G, Lospalluti ML, Penza R, Selvaggi FP, Chiozza ML, Svelto M: Urinary aquaporin 2 and calciuria correlate with the severity of enuresis in children. J Am Soc Nephrol 2000;11:1873–1881.
27 Russ WP, Engelman DM: The GxxxG motif: a framework for transmembrane helix-helix association. J Mol Biol 2000;296:911–919.
28 Kamsteeg EJ, Wormhoudt TA, Rijss JP, van Os CH, Deen PM: An impaired routing of wild-type aquaporin-2 after tetramerization with an aquaporin-2 mutant explains dominant nephrogenic diabetes insipidus. EMBO J 1999;18:2394–2400.
29 Boccalandro C, De Mattia F, Guo DC, Xue L, Orlander P, King TM, Gupta P, Deen PM, Lavis VR, Milewicz DM: Characterization of an aquaporin-2 water channel gene mutation causing partial nephrogenic diabetes insipidus in a Mexican family: evidence of increased frequency of the mutation in the town of origin. J Am Soc Nephrol 2004;15:1223–1231.
30 Meusser B, Hirsch C, Jarosch E, Sommer T: ERAD: the long road to destruction. Nat Cell Biol 2005;7:766–772.
31 Gardner TG, Franklin RA, Robinson PJ, Pederson NE, Howe C, Kearse KP: T cell receptor assembly and expression in the absence of calnexin. Arch Biochem Biophys 2000;378:182–189.
32 Kosuge T, Toyoshima S: Increased degradation of newly synthesized interferon-gamma (IFN-gamma) in anti CD3-stimulated lymphocytes treated with glycoprotein processing inhibitors. Biol Pharm Bull 2000;23:545–548.
33 Murata K, Mitsuoka K, Hirai T, Walz T, Agre P, Heymann JB, Engel A, Fujiyoshi Y: Structural determinants of water permeation through aquaporin-1. Nature 2000;407:599–605.